ELSEVIER

Earth and Planetary Science Letters 197 (2002) 151–164

EPSL

www.elsevier.com/locate/epsl

Laschamp Excursion at Mono Lake?

D.V. Kent [a,b,*], S.R. Hemming [a,c], B.D. Turrin [a]

[a] *Lamont-Doherty Earth Observatory, Columbia University, Rt. 9W, Palisades, NY 10964-0190, USA*
[b] *Department of Geological Sciences, Rutgers University, Piscataway, NJ 08854, USA*
[c] *Department of Earth and Environmental Sciences, Columbia University, Palisades, NY 10964, USA*

Received 10 October 2001; received in revised form 10 January 2002; accepted 11 January 2002

Abstract

The Laschamp Geomagnetic Excursion (ca. 41 ka) and a related increase of cosmogenic nuclides provides a global tie point among sedimentary and ice core records. In the Wilson Creek Formation, Mono Lake, California, the Laschamp Excursion has not been recognized although the so-called Mono Lake excursion was found in the section with an estimated age of about 28 ^{14}C ka. However, our reevaluation of the age of the Mono Lake excursion at its type locality using new ^{14}C dates on carbonates and ^{40}Ar/^{39}Ar sanidine dates on ash layers yields an estimate of 38–41 ka. This chronology and the absence of a second excursion in the Wilson Creek Formation suggest that the distinct paleomagnetic feature with negative inclinations at Mono Lake is correlative with the Laschamp Excursion.

Keywords: magnetic field; C-14; argon; ash; sanidine

1. Introduction

The Laschamp Geomagnetic Excursion was named for anomalous paleomagnetic directions (up to 158° from the expected dipole value) [1] associated with low absolute paleointensities [2,3] in several lava flows from La Chaîne des Puys, Massif Central, France. Deviating directions and/or very low (absolute or relative) paleointensities of approximately the same age (~41 ka, thousands of years before present) as the Laschamp Excursion have been found in Icelandic lavas [4,5] and in numerous deep-sea sediment and lacustrine records [6–11]. At about Laschamp time, there is also a substantial peak in cosmogenic ^{10}Be measured in both Antarctic and Greenland ice cores [12–14] and in deep-sea sediments [15–17]; a coincident peak in cosmogenic ^{36}Cl occurs in the GRIP ice core from Greenland [18]. The increased ^{10}Be and ^{36}Cl fluxes have been attributed to the low geomagnetic intensity associated with the Laschamp Excursion [19,20], which must be considered a global phenomenon. However, cosmogenic ^{10}Be or ^{36}Cl peaks attributed to the ~28 ^{14}C ka Mono Lake excursion have also been reported in some ice cores [21,22] and sedimentary records [23], complicating correlations and interpretations with respect to geomagnetic excursions.

In a search for a record of the Laschamp Excursion in the Great Basin of the western USA, Denham and Cox [24] found an episode of anom-

* Corresponding author.
Tel.: +1-732-445-7049; Fax: +1-732-445-3374.
E-mail address: dvk@ldeo.columbia.edu (D.V. Kent).

0012-821X/02/$ – see front matter
PII: S0012-821X(02)00474-0

alous paleomagnetic secular variation in a freshly cut section of lacustrine sediments of the Wilson Creek Formation at Mono Lake, California [25]. They named this feature the Mono Lake excursion because this record had only steep positive inclinations but not the negative inclinations that characterize the Laschamp Excursion at its type locality. Subsequent work at the Wilson Creek section [26] revealed a new aspect of the Mono Lake excursion that included an episode of low relative paleointensities and negative inclinations resulting in directions more than 100° away from the expected dipole field orientation. The Mono Lake excursion was subsequently documented in several other sedimentary sections from the western USA [27–29], even though negative inclinations may not always be found due to overprinting [30] and other imperfections in the paleomagnetic record [31]. Moreover, elevated ^{10}Be contents in the interval of the Wilson Creek sediments that corresponds to the Mono Lake excursion [32] provide supporting evidence of its global geomagnetic significance. Nevertheless, the Mono Lake excursion was still considered temporally distinct from (although now actually younger than) the Laschamp Excursion, a view that has been accepted almost universally despite dating uncertainties (see review by [33]).

2. Previous dates on Laschamp and Mono Lake excursions

The first published dates on the Laschamp Excursion at its type locality, obtained from ^{14}C and whole rock K–Ar dating, ranged from 8.7 to 20 ka [1]. The Laschamp more than doubled in age when Hall and York [34] obtained whole rock K–Ar and ^{40}Ar/^{39}Ar dates of 47.4 ± 1.9 and 45.4 ± 2.5 ka, and concurrently Gillot et al. [35] obtained K/Ar dates of 43.0 ± 5.0 and 50.0 ± 7.5 ka for the Laschamp and Olby flows, respectively. Thermoluminescence dates range from 32.5 ± 3.1 ka [36] to 44.1 ± 6.5 ka [35]. A ^{14}C measurement on residual humin from a thin organic-rich layer underlying the Olby flow indicated an age of at least 36 ^{14}C ka ($\sim$39.5 calendar ka), the limit of the counting method used [35]. A concordant result of 39 ± 6 ka was obtained with the ^{230}Th/^{238}U disequilibrium method [37]. Dating of the Laschamp Excursion is thus rather uncertain but based on several different chronometers, its age is likely to be within the limits of 39 and 45 ka with a generally accepted nominal age of $\sim$41 ka [11].

The initial estimated age ($\sim$24 ^{14}C ka) for the Mono Lake excursion [24,26] was based on interpolation from just two radiocarbon dates in the Wilson Creek section [25]. An updated $\sim$28 ^{14}C ka estimate [38] for the Mono Lake excursion used a series of 27 published radiocarbon measurements on tufa or ostracodes [39,40]. This age estimate is appreciably different than for the Laschamp Excursion but it does not take into account radiocarbon reservoir effects, or modern carbon contamination effects and radiocarbon production variations, nor has it been tested directly with an independent chronometer.

3. New radiocarbon dates from Mono Lake

We present new radiocarbon data from lacustrine carbonates (ostracodes and tufa nodules) from 11 stratigraphic horizons from the lower 5 m of the Wilson Creek section (Fig. 1). Samples for ^{14}C AMS analysis were disaggregated in deionized water and sieved. Ostracodes or tufa nodules were hand-picked from the >250 μm size fraction. In horizons where there is abundant tufa, it is virtually impossible to find clean shells and this includes much of the interval between 2 and 5 m in the section (Fig. 1, Table 1). Accordingly, we made measurements on pairs of uncoated and tufa-encrusted ostracodes (3.5 m), tufa-encrusted ostracodes and tufa nodules (2.0, 2.5 and 3.1 m) and variably encrusted ostracodes (4.67 m). The more encrusted ostracode or tufa nodule samples gave ages that were always younger (by 780–2160 ^{14}C years) with a general trend of larger age differences in older samples. We consider the greater surface area of the tufa, and thus greater susceptibility to modern carbon contamination, to be a likely explanation for the age differences.

To further address the issue of modern carbon

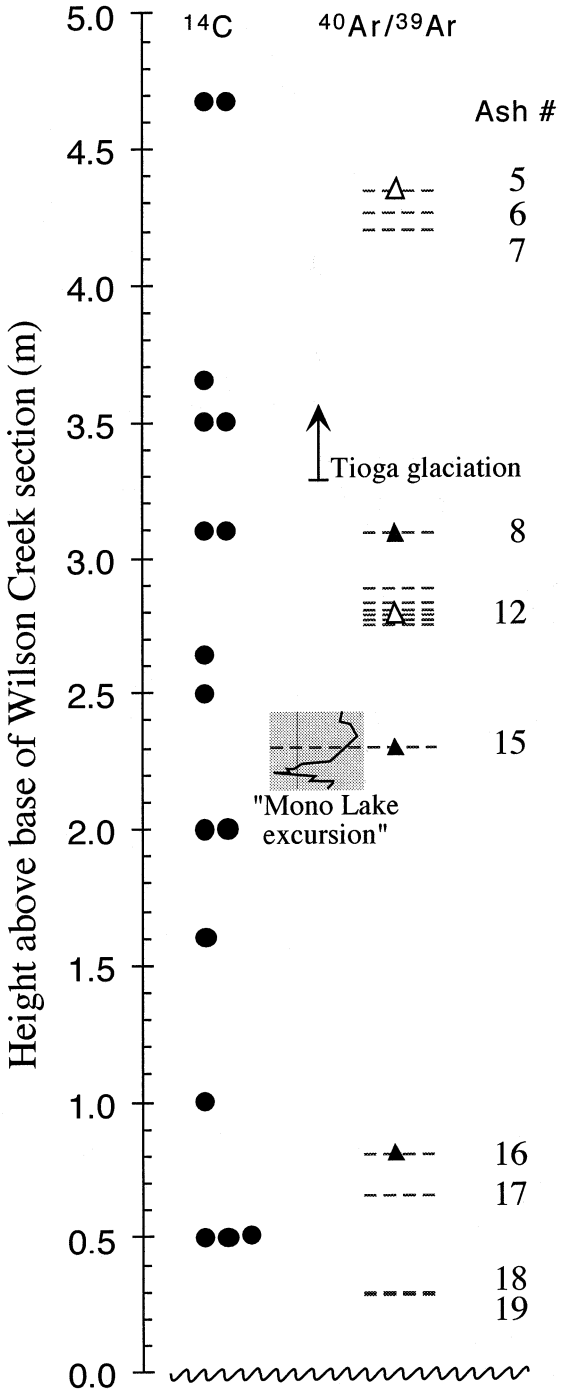

Fig. 1. Schematic stratigraphic section of Wilson Creek Formation at Mono Lake showing sampling levels of carbonate for ^{14}C analysis (from Wilson Creek section) and ash layers for $^{40}Ar/^{39}Ar$ analysis (from south shore section, Ashes #8, 15, 16 analyzed here, Ashes #5 and 12 reported by [52]). Note that Ash #15 is within the Mono Lake excursion [24,26].

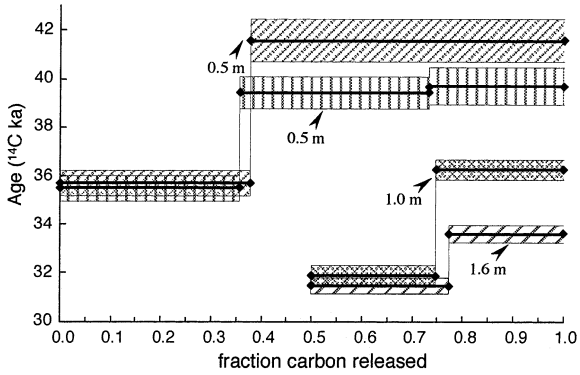

Fig. 2. Results of progressive dissolution of three ostracode samples from the Wilson Creek Formation (I. Hajdas, unpublished data). The patterned areas represent the 1σ analytical uncertainties on the analyses. The sample from 0.5 m was replicated. The fractions are estimated by the pressure of CO_2 evolved as the samples were partially dissolved in the extraction device. We dissolved away 50% of the $CaCO_3$ from the samples from 1.0 and 1.6 m prior to sending them to ETH.

contamination, four sample aliquots were subjected to progressive acid leaching where the apparent age of the fraction of carbon remaining after each leaching step was determined by ^{14}C AMS analysis (Fig. 2). We find significantly younger ages in the first partial dissolution step than in subsequent steps, consistent with absorption of modern carbon on the surfaces (our preferred explanation) or diagenetic overgrowth by younger carbonates. Accordingly, the remainder of the Wilson Creek samples were leached to leave between 22% and 88% of the initial carbonate contents prior to ^{14}C AMS analysis (Table 1). Because a plateau was not always recorded in the progressive dissolution experiments to indicate that the maximum age was achieved (e.g., [41,42]), these ^{14}C dates should be viewed as minimum age constraints.

The differences between the ^{14}C results from residual carbonates that we report here and the bulk carbonate analyses summarized by Benson et al. [38] increase systematically with age. At around the interval of the Mono Lake excursion, there is a 4 kyr difference between our (uncorrected) estimate of 32 ^{14}C ka and the (uncorrected) estimate of 28 ^{14}C ka by Benson et al. [38]; at the base of the lacustrine section, we es-

Table 1
Radiocarbon data from Wilson Creek Formation carbonate samples from Wilson Creek section

ETH	St	Height (m)	Material	^{14}C age[a]	±	δ^{13}C	±	Fraction	Age[b]	Plus[b]	Minus[b]
19 889		0.50	Ostracodes[c]	39 700	790	2.6	1.2	0.268	41 200	3 300	3 340
20 298	8 971	0.50	Ostracodes[d]	41 590	890	2.0	1.2	0.634	42 390	7 500	2 000
21 056	9 915	0.51	Ostracodes	46 100	1 700	0.7	1.2	0.595	45 900	200	2 200
20 190		1.00	Ostracodes[e]	36 250	430	3.4	1.1	0.253	38 350	4 100	3 780
20 191		1.60	Ostracodes[f]	33 610	360	3.0	1.2	0.227	35 610	4 500	1 450
21 419	9 900	2.00	Tufa nodules	31 240	360	6.9	1.2	0.878	33 640	700	2 200
21 420	9 901	2.00	Ostracodes (crusted)	33 400	580	2.1	1.2	0.619	35 600	3 700	1 900
21 421	9 902	2.50	Tufa nodules	29 490	320	3.2	1.2	0.806	32 390	500	2 000
21 422	9 903	2.50	Ostracodes (crusted)	30 510	360	4.0	1.2	0.641	32 710	550	2 300
21 429	9 910	2.64	Ostracodes (crusted)	29 400	290	−1.3	1.2	0.392	31 900	330	2 200
21 423	9 904	3.10	Tufa nodules	26 290	230	4.7	1.2	0.479	28 790	1 200	2 400
21 424	9 905	3.10	Ostracodes (crusted)	27 620	260	2.2	1.2	0.569	30 120	1 000	2 500
21 426	9 907	3.50	Ostracodes (crusted)	23 080	200	3.3	1.2	0.478	25 380	200	2 300
21 427	9 908	3.50	Ostracodes	23 860	240	0.6	1.2	0.515	26 160	900	2 400
21 430	9 911	3.66	Ostracodes (crusted)	23 720	190	5.2	1.2	0.336	25 720	800	2 200
21 431	9 912	4.67	Ostracodes (crusted)	21 170	160	−0.1	1.2	0.457	23 170	400	2 200
21 432	9 913	4.67	Ostracodes (crusted)	20 020	150	1.7	1.2	0.485	22 020	700	2 200

[a] Measured ^{14}C age of residual carbonate, after sequential dissolution within the evacuated extraction device. Measurements were made at ETH, Zurich. No corrections are applied. Leach fraction analyzed is indicated in the column labeled fraction.
[b] Corrected calendar age and assigned uncertainties. 1000 years have been subtracted from the measured values as a first order reservoir correction, although values as high as 2500 years have been found for tufa–wood pairs [43]. The reservoir-corrected ages were then corrected based on published ^{14}C–calendar comparisons in that age range [47,49,50,60] to give the 'Age' estimate. The plus and minus errors are estimated by taking 800 and 2500 year reservoir corrections [43] and adding the minimum published calendar age difference to the 2500 year-corrected value, and the maximum published calendar age difference to the 800 year-corrected value.
[c] Dissolution steps shown in Fig. 3. Recalculated bulk age 37 803.
[d] Dissolution steps shown in Fig. 3. Recalculated bulk age 38 793.
[e] Dissolution steps shown in Fig. 3. Recalculated bulk age 33 768.
[f] Dissolution steps shown in Fig. 3. Recalculated bulk age 32 318.

timate an age greater than 46 ^{14}C ka whereas Benson et al. [38] estimate 36 ^{14}C ka. These differences can be explained by just a slightly higher ($\sim$1%) modern carbon contamination bias in the bulk carbonate ^{14}C data reported by Benson et al. [38]. Our ^{14}C analyses on partially dissolved carbonate are probably not completely free of contamination and are therefore probably still biased to younger ages on this basis alone. With the caveat of potential addition of dead carbon at the time of carbonate crystallization (we subtracted 1000 years from the measured ^{14}C dates as a first order correction for reservoir effects [43–45]; Table 1), a strong case is thus emerging that ^{14}C age estimates from carbonates provide a minimum age of the sample (see also [38,40]). In addition, although the variable ^{14}C production rate is not well calibrated beyond about 20 ka (e.g., [46–51]), the correction of ^{14}C apparent dates to calendar years is expected to be positive by several thousand years (Table 1).

4. ^{40}Ar/^{39}Ar data for ash layers at Mono Lake

The Wilson Creek section contains 19 volcanic ash layers [25] that allow the possibility of using the ^{40}Ar/^{39}Ar dating technique as an independent chronometer [52]. The ashes are numbered #1 to #19 from the top of the section [25]; the Mono Lake excursion is virtually bisected by Ash #15 which can be traced throughout the Mono Basin [26,28]. Although analytically feasible in favorable cases, the Wilson Creek ashes are pushing the young limits of the ^{40}Ar/^{39}Ar dating method, and results can be complicated by extended mag-

ma chamber residence (e.g., [53,54]) or other sources of old inherited ages (e.g., [52,55,56]). Chen et al. [52] reported $^{40}Ar/^{39}Ar$ analyses from individual sanidine crystals from ash layers #5 and 12 in the Wilson Creek Formation from the south shore of Mono Lake. They found a range of sanidine ages in each ash layer but proposed that the youngest populations could be interpreted as the eruption ages because they were generally consistent with ^{14}C ages. For our study, we analyzed sanidine separates from Ashes #8, 15, and 16. The new and published $^{40}Ar/^{39}Ar$ data are shown as isochron plots and ideograms in Fig. 3.

The individual ash layers from the Wilson Creek Formation we studied are well defined with uniform thicknesses on outcrop scale and occur in the same packaging at the south shore and Wilson Creek sections, suggesting there has been little sedimentary reworking. Nevertheless, the ash layers are usually characterized by a wide range of sanidine ages. As an example that is directly pertinent to the age of the Mono Lake excursion, 34 individual sanidine crystals from Ash #15 yielded ages between 49 and 108 ka, a range far exceeding the analytical precision of individual single-grain measurements (Table 2, Fig. 3G,H). The integrated age is 62.7 ± 0.4 ka but is unlikely to represent any particular igneous event since there are distinct subpopulations of sanidine ages. More meaningful is the constraint on the maximum depositional age for Ash #15 as 49.9 ± 0.8 ka, represented by eight of the 34 analyses by selecting the youngest grain and those grains with ages within its analytical uncertainty. By the same argument, the maximum depositional ages for Ashes #5, 12, and 16 are 23.1 ± 1.2 ka, 35.4 ± 2.8 ka, and 51.4 ± 1.0 ka, respectively. The fact that the youngest sanidine age can only be regarded as the maximum depositional age for an ash layer is highlighted by the sobering results from Ash #8. Although stratigraphically above and therefore younger than Ash #12, which has a maximum $^{40}Ar/^{39}Ar$ age of 35.4 ka, all 13 sanidines in the sample from Ash #8 yielded $^{40}Ar/^{39}Ar$ ages between 764 and 810 ka, with an isochron age of 762.9 ± 0.5 ka (Fig. 3C,D). Clearly, the entire measured population of sanidines in the sample from Ash #8 represents contamination from a much earlier event, perhaps by erupting through the nearby Bishop Tuff. More extensive sampling would be needed to isolate any magmatic sanidine associated with this and some of the other eruptions.

5. Age model for Wilson Creek section at Mono Lake

To derive age estimates for the Mono Lake excursion from these data, we have taken three alternative approaches in constructing an age model for the Wilson Creek section (Fig. 4). Although both dating systems are complicated, in this context the ^{14}C dates provide minimum constraints and the $^{40}Ar/^{39}Ar$ dates provide maximum constraints on the age of deposition. According to the published paleomagnetic data [26], the Mono Lake excursion in the Wilson Creek section can be inferred to extend from $\sim$15 cm below to $\sim$15 cm above Ash #15, where the most negative inclination was measured in a sample located 9.9 cm below Ash #15.

Model 1 assumes a constant sedimentation rate of about 19 cm/kyr, calculated by fitting the ^{14}C results between 2 and 4 m in the section (to avoid an apparent ^{14}C age reversal in a subset of seven samples from the interval of 0.61–1.42 m; I. Hajdas, personal communication, 2000). This approach yields minimum ages of 33.7 ka for Ash #15 and 34.2 ka for the diagnostic most negative inclination of the Mono Lake excursion. Model 2 also assumes a constant sedimentation rate, which in this case is $\sim$13 cm/kyr as calculated from a fit to the minimum $^{40}Ar/^{39}Ar$ ages for Ashes #5, 12 and 16. This yields an estimate of 40.2 ka for Ash #15, and 40.8 ka for the most negative inclination of the Mono Lake excursion. Model 3 is a hybrid that assumes a change of sedimentation rate at the beginning of Tioga glaciation (3.3 m, $\sim$29 ka [38]), from about 11 cm/kyr that accommodates the $^{40}Ar/^{39}Ar$ age for Ash #16 and the 46.1 ± 1.7 ^{14}C ka age near the base of the section, to 19 cm/kyr using the ^{14}C-based ages for the upper part of the section as in Model 1. This preferred age model yields an estimate of 37.4 ka for Ash #15 (Table 3) and 38.2 ka for the level

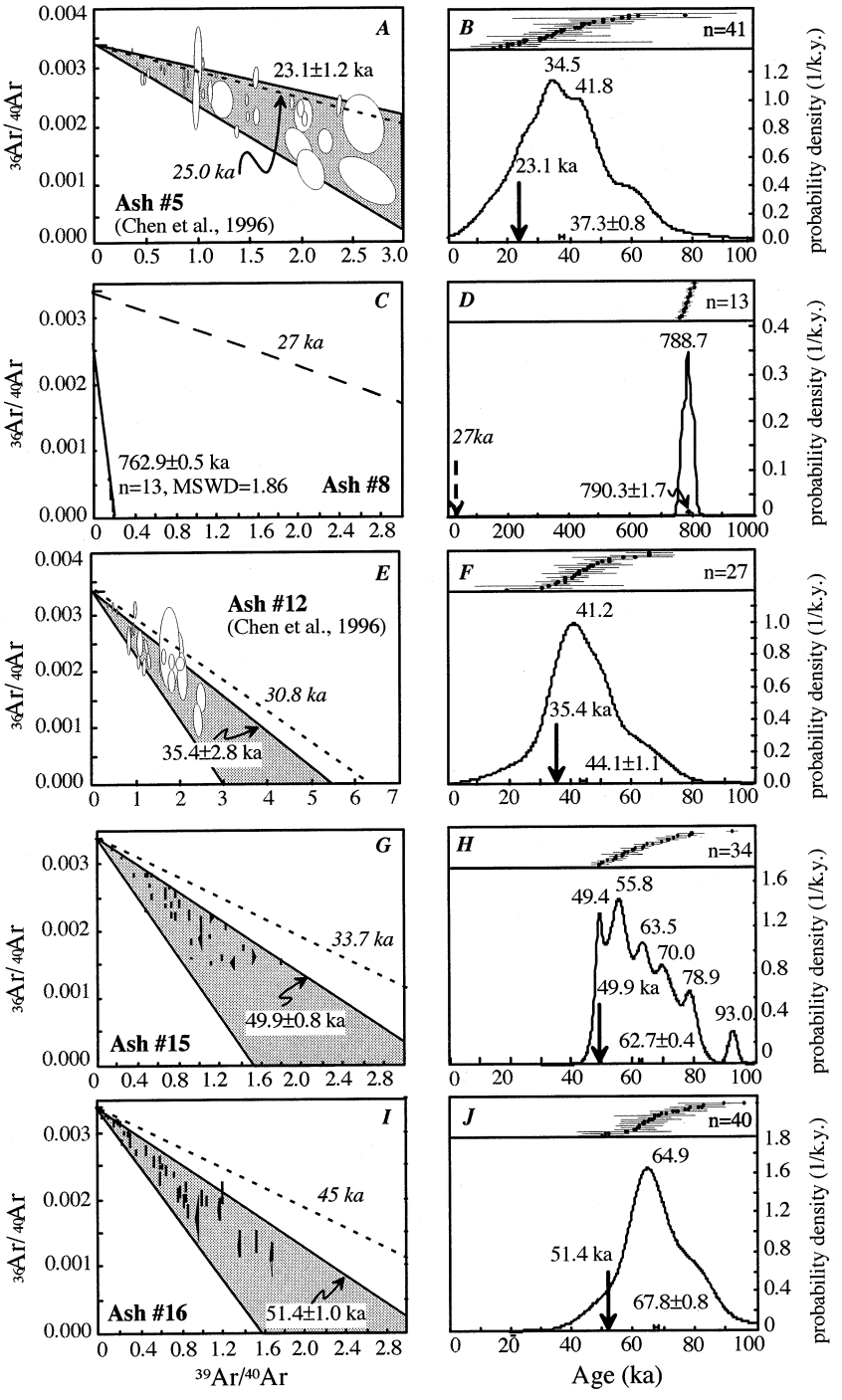
A
23.1±1.2 ka
25.0 ka
Ash #5
(Chen et al., 1996)
B
n=41
34.5
41.8
23.1 ka
37.3±0.8
C
27 ka
762.9±0.5 ka
n=13, MSWD=1.86
Ash #8
D
n=13
788.7
27ka
790.3±1.7
E
Ash #12
(Chen et al., 1996)
30.8 ka
35.4±2.8 ka
F
n=27
41.2
35.4 ka
44.1±1.1
G
33.7 ka
49.9±0.8 ka
Ash #15
H
n=34
49.4
55.8
63.5
70.0
78.9
93.0
49.9 ka
62.7±0.4
I
45 ka
Ash #16
51.4±1.0 ka
J
n=40
64.9
51.4 ka
67.8±0.8
36Ar/40Ar
39Ar/40Ar
probability density (1/k.y.)
Age (ka)

Fig. 3. Isochron plots (left side) and ideograms (right side) of $^{40}Ar/^{39}Ar$ data from Wilson Creek Ashes #5, 8, 12, 15, and 16. In each isochron plot the gray area (sphenochron, terminology of [52]) represents the range of measured ages for the ash, with the minimum population labeled. Dashed line is our ^{14}C-based calendar year estimate as labeled. In the ideogram plots, the vertical arrow marks the youngest population, except in D where the age of Ash #8 is estimated by interpolation between ashes #5 and 12. (A,B) Isochron plot and ideogram for Ash #5. Data from Chen et al. [52]. (C,D) Isochron plot (age calculated from all 13 sanidine analyses) and ideogram for Ash #8. (E,F) Isochron plot and ideogram for Ash #12. Data from Chen et al. [52]. (G,H) Isochron plot (age calculated from eight of 34 analyses) and ideogram for Ash #15. (I,J) Isochron plot (age calculated from five of 40 analyses) and ideogram for Ash #16.
←

of most negative inclination of the Mono Lake excursion. Note that the ^{14}C dates can be reconciled to Model 3 by assuming a very small residual bias of 0.5–1.5% modern carbon contamination in our carbonate ^{14}C data (Fig. 4).

6. Implications of age model for 'Mono Lake excursion'

We conclude that the Mono Lake excursion at the Wilson Creek type locality is older than 34.2 ka based on interpolation of ^{14}C data taken at face value and younger than 49.9 ka based on the youngest population of sanidines in Ash #15, and most probably occurred somewhere between 38 and 41 ka. These age limits overlap the best available age constraints for the Laschamp excursion at its type locality as discussed above (Fig. 4). Lacking a distinguishable difference in age, the paleomagnetic feature that has heretofore been identified as the Mono Lake excursion at Wilson Creek should most logically be regarded as a record of the Laschamp Excursion. Indirect support for this conclusion is the absence of a second geomagnetic excursion that might otherwise be identified as the Laschamp in the published paleomagnetic records from below (as well as above) the Mono Lake feature at Wilson Creek [24,26,39], even though the lacustrine section is now documented to extend to at least 46 ^{14}C ka and thus encompassing the age constraints ($\sim$35 ^{14}C ka in North Atlantic sediment cores [49]) of the Laschamp Excursion.

In detailed paleomagnetic records from North Atlantic sediment cores placed on the GISP2 time scale, negative inclinations associated with the Laschamp Excursion occur over only $\sim$1500 years and correspond to a marked decrease in geomagnetic paleointensity in the NAPIS-75 stacked record at $\sim$41 ka [9,11]. A similar picture emerges for the published paleomagnetic record for the Wilson Creek section using our new age constraints: the short interval of negative inclinations just below Ash #15 corresponds to a decrease in relative paleointensity at an estimated age of $\sim$39 ka, which we do not regard as significantly different from the GISP2 age estimate of $\sim$41 ka for the Laschamp Excursion (Fig. 5). No other interval with reproducible negative inclinations has been documented from at least 30 to 50 ka in the recent study of North Atlantic cores [9] (but see also [57]) or from 13 ka to the base of the Wilson Creek section [26,39], which we estimate is at least 46 ^{14}C ka.

A major peak in the flux of cosmogenic isotopes is observed in ice core and sediment records [12–16,20,58] and has been linked to very low geomagnetic intensities associated with the Laschamp Excursion [17]. A second, younger peak in cosmogenic isotopes has also been identified in some ice core and sediment records and attributed to the Mono Lake excursion [22,23,49]. This subsidiary cosmogenic isotope peak may very well be associated with low geomagnetic intensities observed at around 34 ka in the NAPIS-75 record (Fig. 5); however, it should not be identified with the Mono Lake excursion which we have shown is not distinguishable in age at its type locality from the Laschamp Excursion that has priority in nomenclatural usage.

Highly divergent directions taken as evidence of geomagnetic excursions are invariably associated with major decreases in paleointensity (DIPs), which must involve the global dipole field [6]. A case in point is the Laschamp Excursion. However, the converse often does not hold so that a DIP may not always be associated with divergent

Table 2
$^{40}Ar/^{39}Ar$ data from individual sanidine crystals from volcanic ashes in Wilson Creek Formation collected from the south shore of Mono Lake[a]

Sample[b]	Ca/K	$^{36}Ar/^{39}Ar$	$^{40}Ar^*/^{39}Ar$	Mol ^{40}Ar	Mol ^{39}Ar	% $^{40}Ar^*$	Age (ka)	±
Ash #8								
10388-01	0.0224	0.00337	5.019	3.4E-14	5.9E-15	83.5	808.5	3.9
10388-02	0.0201	0.00219	4.960	1.9E-14	3.5E-15	88.5	799.0	5.8
10388-03	0.0205	0.00185	4.898	2.2E-14	4.2E-15	90.0	788.9	3.9
10388-05	0.0188	0.00210	4.959	2.4E-15	2.7E-16	88.9	798.6	7.7
10388-06	0.0236	0.00198	5.028	1.2E-14	2.3E-15	89.6	810.0	9.2
10388-07	0.0180	0.00288	4.890	2.2E-14	4.2E-15	85.2	787.6	7.4
10388-08	0.0183	0.00130	4.813	1.2E-14	2.1E-15	92.6	775.4	6.7
10388-09	0.0155	0.00170	4.937	9.8E-15	2.0E-15	90.8	795.1	7.6
10388-10	0.0115	0.00093	4.781	1.2E-14	2.2E-15	94.5	770.0	6.8
10388-11	0.0118	0.00087	4.877	1.3E-14	2.6E-15	95.0	785.5	7.4
10388-13	0.0194	0.00218	4.792	9.9E-15	2.0E-15	88.1	771.9	9.6
10388-14	0.0208	0.00069	4.858	8.5E-16	2.3E-16	96.0	782.4	7.4
10388-15	0.0232	0.00135	4.744	9.0E-15	1.7E-15	92.3	764.2	6.5
Ash #15								
10386-01	0.0161	0.01272	0.365	6.0E-14	1.5E-14	8.8	58.7	3.3
10386-03	0.0145	0.00216	0.352	4.7E-15	4.8E-15	35.6	56.8	1.7
10386-04	*0.0144*	*0.00085*	*0.306*	*3.1E-15*	*5.4E-15*	*55.0*	*49.3*	*0.9*
10386-08	0.0186	0.00133	0.492	3.6E-15	4.0E-15	55.6	79.1	1.6
10386-09	*0.0162*	*0.00371*	*0.306*	*7.6E-15*	*5.4E-15*	*21.9*	*49.5*	*1.9*
10386-12	*0.0144*	*0.00563*	*0.336*	*8.5E-15*	*4.2E-15*	*16.8*	*54.2*	*2.5*
10386-13	0.0180	0.02284	0.355	3.0E-14	4.3E-15	5.0	57.2	6.3
10386-16	0.0166	0.00173	0.577	4.9E-15	4.5E-15	53.1	92.9	1.4
10386-20	*0.0138*	*0.00530*	*0.313*	*7.3E-15*	*3.9E-15*	*16.6*	*50.3*	*2.8*
10386-21	*0.0134*	*0.00122*	*0.340*	*1.5E-15*	*2.1E-15*	*48.6*	*54.6*	*1.9*
10386-22	0.0166	0.00379	0.341	3.8E-15	2.6E-15	23.4	55.1	2.8
10386-25	0.0158	0.00488	0.673	5.5E-15	2.6E-15	31.8	108.4	3.1
10386-26	0.0154	0.00105	0.343	1.9E-15	2.9E-15	52.5	55.3	2.0
10386-27	0.0141	0.00594	0.360	6.6E-15	3.1E-15	17.0	58.1	3.2
10386-30	0.0163	0.00174	0.395	3.2E-15	3.5E-15	43.4	63.7	1.7
10386-33	0.0143	0.00350	0.446	4.5E-15	3.0E-15	30.1	71.8	2.5
10386-34	0.0143	0.00206	0.376	1.7E-15	1.7E-15	38.2	60.4	2.9
10386-35	0.0145	0.00514	0.405	3.2E-15	1.7E-15	21.1	65.2	3.7
10386-36	0.0141	0.00326	0.406	2.8E-15	2.0E-15	29.7	65.4	3.2
10386-37	0.0167	0.00755	0.458	5.2E-15	1.9E-15	17.0	73.8	4.1
10386-38	0.0184	0.00196	0.496	2.5E-15	2.3E-15	46.2	80.0	2.5
10386-39	0.0133	0.00114	0.417	2.3E-15	3.0E-15	55.4	67.1	1.9
10386-40	*0.0137*	*0.00326*	*0.324*	*3.0E-15*	*2.3E-15*	*25.2*	*52.0*	*3.0*
10386-41	*0.0136*	*0.00195*	*0.310*	*1.5E-15*	*1.7E-15*	*35.0*	*49.9*	*2.4*
10386-42	0.0153	0.00184	0.445	1.5E-15	1.5E-15	45.1	71.8	2.9
10386-43	0.0246	0.00129	0.434	2.7E-15	3.2E-15	53.3	69.9	1.7
10386-44	0.0124	0.00369	0.378	2.1E-15	1.4E-15	25.7	60.9	3.8
10386-45	0.0129	0.00286	0.449	1.9E-15	1.5E-15	34.7	72.3	3.5
10386-46	0.0131	0.00296	0.357	2.4E-15	1.9E-15	29.0	57.6	3.0
10386-47	*0.0204*	*0.00162*	*0.316*	*1.9E-15*	*2.4E-15*	*39.8*	*50.8*	*2.1*
10386-48	0.0143	0.00466	0.494	3.8E-15	2.0E-15	26.4	79.6	4.2
10386-49	0.0240	0.00301	0.468	2.4E-15	1.8E-15	34.5	75.3	3.2
10386-50	0.0164	0.00199	0.397	2.1E-15	2.1E-15	40.3	64.1	2.0
10386-51	0.0134	0.00245	0.381	1.5E-15	1.3E-15	34.5	61.3	3.6

Table 2 (*Continued*).

Sample[b]	Ca/K	$^{36}Ar/^{39}Ar$	$^{40}Ar^*/^{39}Ar$	Mol ^{40}Ar	Mol ^{39}Ar	% $^{40}Ar^*$	Age (ka)	±
Ash #16								
10387-01	*0.0140*	*0.01504*	*0.321*	*2.6E-14*	*5.5E-15*	*6.7*	*51.6*	*6.2*
10387-02	0.0150	0.01098	0.598	1.7E-14	4.3E-15	15.6	96.4	8.8
10387-03	0.0152	0.01079	0.418	4.3E-14	1.2E-14	11.6	67.3	5.2
10387-04	0.0133	0.00417	0.380	1.2E-14	7.4E-15	23.6	61.1	4.1
10387-05	0.0162	0.00385	0.407	1.6E-14	1.1E-14	26.4	65.6	2.7
10387-06	*0.0156*	*0.01315*	*0.320*	*2.5E-14*	*6.0E-15*	*7.6*	*51.6*	*7.2*
10387-08	0.0144	0.00392	0.430	8.2E-14	3.8E-15	27.1	69.3	2.6
10387-09	0.0148	0.00310	0.397	1.5E-14	9.7E-15	30.3	64.1	3.4
10387-10	0.0155	0.00354	0.414	5.4E-15	4.1E-15	28.4	66.7	4.5
10387-11	0.0186	0.00694	0.513	7.2E-15	4.9E-15	20.0	82.6	4.3
10387-12	0.0156	0.00183	0.387	2.6E-14	1.0E-14	41.7	62.4	3.8
10387-13	0.0129	0.00255	0.479	4.5E-15	4.8E-15	38.9	77.2	6.1
10387-14	0.0137	0.00230	0.484	4.4E-15	3.5E-15	41.7	78.1	5.7
10387-15	0.0137	0.02553	0.363	3.7E-15	3.1E-15	4.6	58.5	13.7
10387-17	0.0116	0.00450	0.427	2.7E-14	3.4E-15	24.3	68.8	7.8
10387-18	0.0153	0.00920	0.388	5.4E-13	1.2E-14	12.5	62.4	7.1
10387-20	0.0124	0.00100	0.418	5.5E-15	3.1E-15	58.6	67.3	4.1
10387-21	0.0151	0.00227	0.456	1.6E-14	5.0E-15	40.5	73.3	3.8
10387-22	0.0120	0.01780	0.419	2.9E-15	4.1E-15	7.4	67.5	12.8
10387-23	0.0145	0.00244	0.403	4.2E-15	3.7E-15	35.8	65.0	4.4
10387-24	0.0124	0.04250	0.559	1.4E-14	2.4E-15	4.3	89.9	14.5
10387-25	0.0175	0.00867	0.412	5.3E-15	4.7E-15	13.9	66.2	9.6
10387-26	*0.0142*	*0.01435*	*0.326*	*4.1E-14*	*3.1E-15*	*7.1*	*52.5*	*9.9*
10387-27	0.0137	0.00455	0.426	8.2E-15	2.8E-15	24.1	68.6	5.4
10387-28	*0.0127*	*0.03171*	*0.360*	*9.3E-15*	*2.0E-15*	*3.7*	*58.1*	*12.2*
10387-29	0.0114	0.00093	0.443	4.8E-15	2.7E-15	61.7	71.4	5.3
10387-30	0.0134	0.00256	0.464	5.2E-14	5.3E-15	38.0	74.6	5.4
10387-31	0.0135	0.00361	0.519	1.1E-15	1.6E-15	32.7	83.4	5.0
10387-32	0.0172	0.00197	0.387	4.4E-15	3.6E-15	39.9	62.4	3.7
10387-33	0.0148	0.00832	0.465	7.9E-15	4.9E-15	15.9	74.8	8.9
10387-34	0.0125	0.00202	0.518	3.6E-15	3.6E-15	46.4	83.4	5.7
10387-35	0.0125	0.00561	0.393	8.2E-15	2.8E-15	19.2	63.2	7.1
10387-36	0.0125	0.00376	0.489	3.3E-15	2.9E-15	30.6	78.7	4.9
10387-37	0.0122	0.00172	0.505	7.4E-15	3.6E-15	49.9	81.3	8.5
10387-38	0.0124	0.00088	0.385	2.8E-15	1.7E-15	59.7	61.9	4.9
10387-39	0.0105	0.00192	0.396	2.1E-15	2.1E-15	41.1	63.9	5.2
10387-40	*0.0113*	*0.00170*	*0.311*	*1.9E-15*	*3.0E-15*	*38.3*	*50.1*	*6.7*
10387-41	0.0109	0.00153	0.378	2.6E-15	2.7E-15	45.5	60.9	6.4
10387-42	0.0122	0.00064	0.399	1.5E-15	1.8E-15	68.0	64.3	7.3
10387-43	0.0157	0.00198	0.379	1.9E-15	2.3E-15	39.4	61.1	3.7

[a] Samples were co-irradiated with Cobb Mountain sanidine [61] for 20 min at Oregon State University reactor; *J*-value was determined to be 8.645E-5 ± 1.559E-7. Measurements were made in the Ar geochronology lab at LDEO. Ages were calculated from Ar isotope ratios corrected for mass discrimination, interfering nuclear reactions, procedural blanks, and atmospheric Ar contamination.

[b] Italicized samples were used to calculate the age of the minimum populations for Ashes #15 and 16.

directions whose occurrence may depend on the relative magnitude and local configuration of the non-dipole field as well as the fidelity of the magnetic record. The DIP at 34 ka, which is typically not as pronounced as the DIP associated with the Laschamp Excursion at 41 ka [11], is an example of a geomagnetic feature with a more ephemeral expression in paleomagnetic directions (e.g., [9,57]). DIPs are clearly a key element for the interpretation of geomagnetic excursions as well

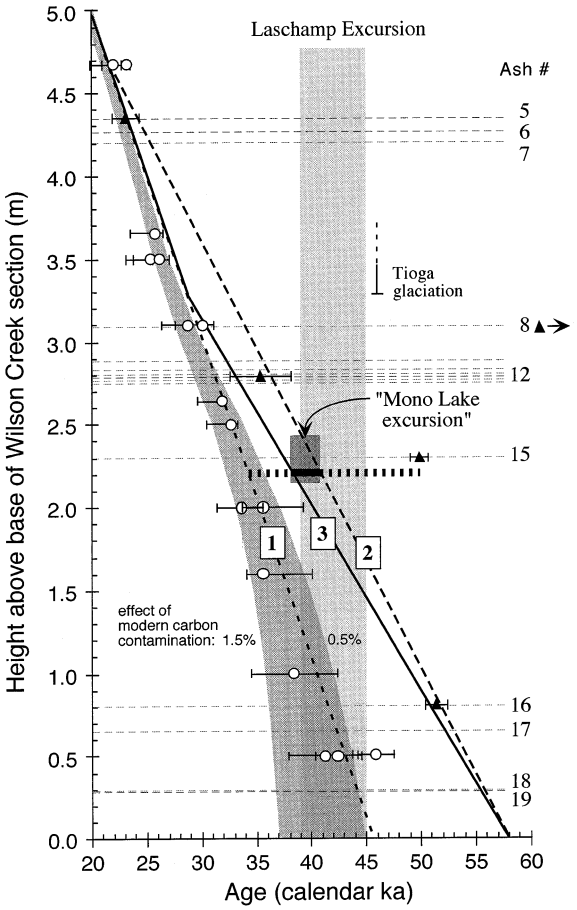

Fig. 4. Geochronological constraints for the Wilson Creek Formation. Horizontal dashed lines, labeled at right, are the locations of the ash layers at the type locality [25]. Radiocarbon data (open circles) are from residual carbonate materials after removing between 12 and 78% in the extraction apparatus (Table 1). $^{40}Ar/^{39}Ar$ data (black triangles) are from the youngest population of measured individual sanidines (Table 2, Fig. 3) and represent the maximum age of the ashes that contain them. Solid and dashed lines labeled 1, 2, and 3 are three sedimentation rate models based on the ^{14}C and $^{40}Ar/^{39}Ar$ data (see text for description). Shaded sinuous area corresponds to the calculated effect of residual bias from 0.5 to 1.5% modern carbon contamination applied to Model 3 estimates. Age estimates for the Mono Lake excursion at Mono Lake, shown by solid bar (most probable) and dashed bar (extrema) for the interval with negative inclinations, are compared to the Laschamp Excursion at Olby/Laschamp estimated as 39–45 ka (see text) and shown by shaded bar.

as being of fundamental importance for assessing geomagnetic modulation of cosmogenic isotope production rates. A separate identification scheme for paleointensity highs and lows might therefore be useful for correlation. For example, using the NAPIS-75 record as a template, the DIPs at 34 ka and 41 ka could be referred to as p5 and p7, respectively, and the bracketing paleointensity highs as p4, p6 and p8, and so forth as illustrated in Fig. 5, reserving p2 for the paleointensity high at ~2 ka and p1 for the subsequent decrease to the present according to archeomagnetic records [59].

One broader implication of our revised overall chronology of the Wilson Creek section concerns the correlation of lake level variations in the Mono Lake basin and Heinrich events in the North Atlantic. Benson et al. [38] found four $\delta^{18}O$ peaks (L1–L4) that they interpreted to represent persistent dry intervals of ~1–2 kyr duration. The youngest peaks (L1 and L2) appear to be reasonably correlated with Heinrich events H1 and H2. Due to uncertainties in the chronology, they were unable to find a correlation for L3 but suggested that L4 might correlate to H4. Our proposed age model for the Wilson Creek Formation would suggest correlation of L3 with H4 (~38 ka) and L4 with H5 (~45 ka) although the age interpretation for L4 is much less certain with the

Table 3
Estimated ages of volcanic ash layers in Wilson Creek Formation based on age Model 3 in Wilson Creek section

Ash #	Age (ka)
5	23.6
6	24.0
7	24.3
8	30.4
9	32.2
10	32.7
11	32.9
12	33.1
13	33.3
14	33.5
15	37.4
16	50.8
17	52.1
18	55.3
19	55.4

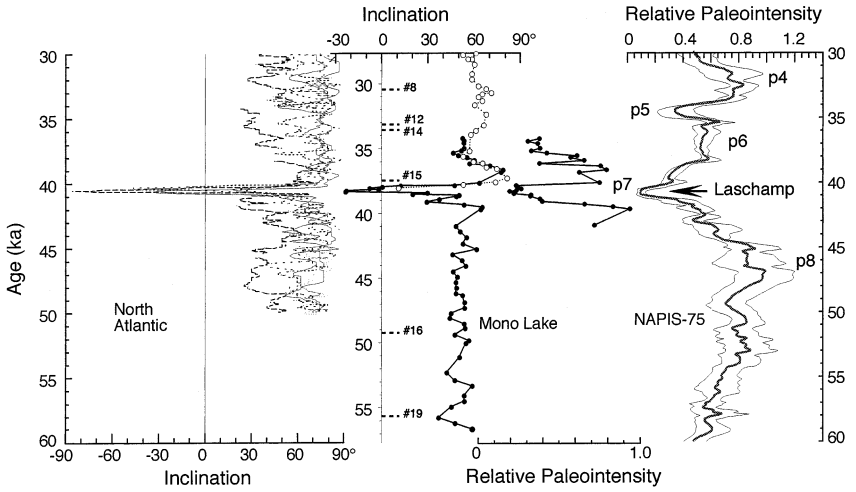

Fig. 5. Comparison of paleomagnetic inclination and relative paleointensity records in the interval encompassing the Laschamp Geomagnetic Excursion from North Atlantic sediment cores (left, inclinations from six cores [9]; right, NAPIS-75 paleointensity stack of six cores showing $\pm 2\sigma$ uncertainty envelope [11] with prominent highs and lows labeled p4, p5, etc.), and from the Wilson Creek Formation at Mono Lake, California (solid circles and lines are inclination and normalized relative paleointensity data for below ash layer #14 tabulated in [26], open circles and dashed lines are inclination data scanned from figure 2 in [39]). The North Atlantic records are placed on a GISP2 time scale [9,11]. The Mono Lake record was converted to age using our age Model 3 and shifted $\sim$2.5 kyr older to optimize the match of the inclination records with the North Atlantic. Positions of ash layers #8, 12, 14, 15, 16, and 19 in Wilson Creek section are shown for reference.

available data. This alternative correlation is also consistent with the first order features of geomagnetic paleosecular variation in these regions, most obvious being the match of the intervals of low relative paleointensity and negative inclination associated with the Laschamp Excursion (Fig. 5). Nevertheless, our hypothesis can be refuted if sanidines significantly younger than the $\sim$41 ka age of the Laschamp Excursion are eventually found in ash layers at or below the 'Mono Lake excursion' in the western USA.

Acknowledgements

We thank Scott Stine for taking us to the south shore section, Gary Hemming and Paul Tomascak for help in the field, Wally Broecker for supporting the ^{14}C analyses, and all for stimulating discussions. Larry Benson kindly provided listings of $CaCO_3$ and ^{18}O data from the Wilson Creek section, Norm Evensen provided the $^{40}Ar/^{39}Ar$ data for Ashes #5 and 12, and Carlo Laj and Catherine Kissel promptly responded to our requests for digital copies of the NAPIS-75 paleointensity and inclination data. We also thank Millie Mendelson for picking the carbonate samples for ^{14}C analyses and Irka Hajdas for making the measurements, Susan Zimmerman for discussions about the Wilson Creek sediments, and Julie Carlut for constructive criticisms of the manuscript. Seed money for this project was obtained from the Lamont Climate Center. Thanks go to Norm Evensen, Chris Hall, and Cor Langereis for their constructive journal reviews. Lamont-Doherty Earth Observatory contribution #6289.*[RV]*

References

[1] N. Bonhommet, J. Zahringer, Paleomagnetism and potassium argon age determinations of the Laschamp geomagnetic polarity event, Earth Planet. Sci. Lett. 6 (1969) 43–46.

[2] A. Chauvin, R.A. Duncan, N. Bonhommet, S. Levi, Paleointensity of the Earth's magnetic field and K-Ar dating of the Louchadiere volcanic flow (central France): New

evidence for the Laschamp Excursion, Geophys. Res. Lett. 16 (1989) 1189–1192.
[3] P. Roperch, N. Bonhommet, S. Levi, Paleointensity of the Earth's magnetic field during the Laschamp excursion and its geomagnetic implications, Earth Planet. Sci. Lett. 88 (1988) 209–219.
[4] S. Levi, H. Audunsson, R.A. Duncan, L. Kristjansson, P.-Y. Gillot, S.P. Jakobsson, Late Pleistocene geomagnetic excursion in Icelandic lavas: confirmation of the Laschamp excursion, Earth Planet. Sci. Lett. 96 (1990) 443–457.
[5] M. Marshall, A. Chauvin, N. Bonhommet, Preliminary paleointensity measurements and detailed magnetic analyses of basalts from the Skalamaelifell excursion, southwest Iceland, J. Geophys. Res. 93 (1988) 11681–11698.
[6] Y. Guyodo, J.-P. Valet, Global changes in intensity of the Earth's magnetic field during the past 800 kyr, Nature 399 (1999) 249–252.
[7] S. Marco, H. Ron, M.O. McWilliams, M. Stein, High-resolution record of geomagnetic secular variation from Late Pleistocene Lake Lisan sediments (paleo Dead Sea), Earth Planet. Sci. Lett. 161 (1998) 145–160.
[8] A.H.L. Voelker, M. Sarnthein, P.M. Grootes, H. Erlenkeuser, C. Laj, A. Mazaud, M.-J. Nadeau, M. Schleicher, Correlation of marine ^{14}C ages from the Nordic sea with the GISP2 isotope record Implications for ^{14}C calibration beyond 25 ka BP, Radiocarbon 40 (1998) 517–534.
[9] C. Kissel, C. Laj, L. Labeyrie, T. Dokken, A. Voelker, D. Blamart, Rapid climatic variations during marine isotopic stage 3 magnetic analysis of sediments from Nordic Seas and North Atlantic, Earth Planet. Sci. Lett. 171 (1999) 489–502.
[10] J.S. Stoner, J.E.T. Channell, C. Hillaire-Marcel, C. Kissel, Geomagnetic paleointensity and environmental record from Labrador Sea core MD95-2024 global marine sediment and ice core chronostratigraphy for the last 110 kyr, Earth Planet. Sci. Lett. 183 (2000) 161–177.
[11] C. Laj, C. Kissel, A. Mazaud, J.E.T. Channell, J. Beer, North Atlantic paleointensity stack since 75 ka (NAPIS-75) and the duration of the Laschamp event, Phil. Trans. R. Soc. London A 258 (2000) 1009–1025.
[12] G.M. Raisbeck, F. Yiou, D. Bourles, C. Lorius, J. Jouzel, N.I. Barkov, Evidence for two intervals of enhanced ^{10}Be deposition in Antarctic ice during the last glacial period, Nature 326 (1987) 273–277.
[13] G.M. Raisbeck, F. Yiou, J. Jouzel, J.R. Petit, N.I. Barkov, E. Bard, ^{10}Be deposition at Vostok, Antarctica during the last 50,000 years and its relationship to possible cosmogenic production variations during this period, in: E. Bard, W.S. Broecker (Eds.), The Last Deglaciation: Absolute and Radiocarbon Chronologies, Springer-Verlag, New York, 1992, pp. 127–140.
[14] F. Yiou, G.M. Raisbeck, S. Baumgartner, J. Beer, C. Hammer, S. Johnsen, J. Jouzel, P.W. Kubik, J. Lestringuez, M. Stievenard, M. Suter, P. Yiou, Beryllium-10 in the Greenland Ice Core Project ice core at Summit, Greenland, J. Geophys. Res. 102 (1997) 26783–26794.
[15] G.C. Castagnoli, A. Albrecht, J. Beer, G. Bonino, C. Shen, E. Callegari, C. Taricco, B. Dittrich-Hannen, P. Kubik, M. Suter, G.M. Zhu, Evidence for enhanced ^{10}Be deposition in Mediterranean sediments 35 kyr BP, Geophys. Res. Lett. 22 (1995) 707–710.
[16] A. Aldahan, G. Possnert, A high-resolution ^{10}Be profile from deep sea sediment covering the last 70 Ka Indication for globally synchronized environmental events, Quat. Geochronol. 17 (1998) 1023–1032.
[17] C. Robinson, G.M. Raisbeck, F. Yiou, B. Lehman, C. Laj, The relationship between ^{10}Be and geomagnetic field strength records in central North Atlantic sediments during the last 80 ka, Earth Planet. Sci. Lett. 136 (1995) 551–557.
[18] S. Baumgartner, J. Beer, M. Suter, H.-A. Dittrich-Hannen, H.-A. Synal, P.W. Kubik, C. Hammer, S. Johnsen, ^{36}Cl fallout in the Summit Greenland Ice Core Project ice core, J. Geophys. Res. 102 (1997) 26659–26662.
[19] A. Mazaud, C. Laj, M. Bender, A geomagnetic chronology for Antarctic ice accumulation, Geophys. Res. Lett. 21 (1994) 337–340.
[20] S. Baumgartner, J. Beer, J. Masarik, G. Wagner, L. Meynadier, H.-A. Synal, Geomagnetic modulation of the ^{36}Cl flux in the GRIP Ice Core, Greenland, Science 279 (1998) 1330–1332.
[21] J. Beer, S.J. Johnsen, G. Bonani, R.C. Finkel, C.C. Langway, H. Oeschger, B. Stauffer, M. Suter, W. Woelfli, ^{10}Be peaks as time markers in polar ice cores, in: E. Bard, W.S. Broecker (Eds.), The Last Deglaciation: Absolute and Radiocarbon Chronologies, Springer-Verlag, New York, 1992, pp. 141–153.
[22] G. Wagner, J. Beer, C. Laj, C. Kissel, J. Masarik, R. Muscheler, H.-A. Synal, Chlorine-36 evidence for the Mono Lake event in the Summit GRIP ice core, Earth Planet. Sci. Lett. 181 (2000) 1–6.
[23] L.R. McHargue, P.E. Damon, D.J. Donahue, Enhanced cosmic-ray production of ^{10}Be coincident with the Mono Lake and Laschamp geomagnetic excursions, Geophys. Res. Lett. 22 (1995) 659–662.
[24] C.R. Denham, A. Cox, Evidence that the Laschamp polarity event did not occur 13,300–34,000 years ago, Earth Planet. Sci. Lett. 13 (1971) 181–190.
[25] K.R. Lajoie, Quaternary Stratigraphy and Geologic History of Mono Basin, Eastern California, Ph.D. Thesis, University of California, Berkeley, CA, 1968.
[26] J.C. Liddicoat, R.S. Coe, Mono Lake geomagnetic excursion, J. Geophys. Res. 84 (1979) 261–271.
[27] R.M. Negrini, J.O. Davis, K.L. Verosub, Mono Lake geomagnetic excursion found at Summer Lake, Oregon, Geology 12 (1984) 643–646.
[28] J.C. Liddicoat, Mono Lake Excursion in Mono Basin, California, and at Carson Sink and Pyramid Lake, Nevada, Geophys. J. Int. 108 (1992) 442–452.
[29] J.C. Liddicoat, Mono Lake Excursion in the Lahontan Basin, Nevada, Geophys. J. Int. 125 (1996) 630–635.

[30] R.S. Coe, J.C. Liddicoat, Overprinting of natural magnetic remanence in lake sediments by a subsequent high-intensity field, Nature 367 (1994) 57–59.
[31] R.L. Hanna, K.L. Verosub, A review of lacustrine paleomagnetic records from western North America 0–40 000 years BP, Phys. Earth Planet. Inter. 56 (1989) 76–95.
[32] T. Ticich, L. Lundberg, D.K. Pal, C.M. Smith, G.F. Herzog, R.K. Moniot, C. Tuniz, W. Savin, T.H. Kruse, J.C. Liddicoat, ^{10}Be contents of Mono Lake sediments search for enhancement during a geomagnetic excursion, Geophys. J. R. Astron. Soc. 87 (1986) 487–492.
[33] J.A. Jacobs, Reversals of the Earth's Magnetic Field, Cambridge University Press, Cambridge, 1994, 346 pp.
[34] C.M. Hall, D. York, K-Ar and ^{40}Ar/^{39}Ar age of the Laschamp geomagnetic polarity reversal, Nature 274 (1978) 462–464.
[35] P.Y. Gillot, J. Labeyrie, C. Laj, G. Valladas, G. Guerin, G. Poupeau, G. Delibrias, Age of the Laschamp paleomagnetic excursion revisited, Earth Planet. Sci. Lett. 42 (1979) 444–450.
[36] G. Guerin, G. Valladas, Thermo-luminescence dating of volcanic plagioclases, Nature 286 (1980) 697–699.
[37] M. Condomines, Age of the Olby-Laschamp geomagnetic polarity event, Nature 276 (1978) 257–258.
[38] L.V. Benson, S.P. Lund, J.W. Burdett, M. Kashgarian, T.P. Rose, J.P. Smoot, M. Schwartz, Correlation of Late Pleistocene lake-level oscillations in Mono Lake, California, with North Atlantic climate events, Quat. Res. 49 (1998) 1–10.
[39] S.P. Lund, J.C. Liddicoat, K.L. Lajoie, T.L. Henyey, S. Robinson, Paleomagnetic evidence for long-term 10^4 year memory and periodic behavior in the Earth's core dynamo process, Geophys. Res. Lett. 15 (1988) 1101–1104.
[40] L.V. Benson, D.R. Currey, R.I. Dorn, K.R. Lajoie, C.G. Oviatt, S.W. Robinson, G.I. Smith, S. Stine, Chronology of expansion and contraction of four Great Basin lake systems during the past 35,000 years, Palaeogeogr. Palaeoclimatol. Palaeoecol. 78 (1990) 241–286.
[41] G.S. Burr, R.L. Edwards, D.J. Donahue, E.R.M. Druffel, F.W. Taylor, Mass spectrometric ^{14}C and U-Th measurements in coral, Radiocarbon 34 (1992) 611–618.
[42] Y. Yokoyama, T.M. Esat, K. Lambeck, L.K. Fifield, Last ice age millenial scale climate changes recorded in Huon Peninsula corals, Radiocarbon 42 (2000) 384–401.
[43] W.S. Broecker, R. Wanninkhof, G. Mathiew, T.H. Peng, S. Stine, S. Robinson, A. Herczed, M. Stuiver, The radiocarbon budget for Mono Lake – an unsolved mystery, Earth Planet. Sci. Lett. 88 (1988) 16–26.
[44] J.C. Lin, W.S. Broecker, R.F. Anderson, J.L. Rubenstone, S. Hemming, G. Bonani, New ^{230}Th/U and ^{14}C ages from Lake Lahonton carbonates, Nevada, USA, and a discussion of the origin of initial thorium, Geochim. Cosmochim. Acta 60 (1996) 2817–2832.
[45] W.S. Broecker, A. Walton, The geochemistry of ^{14}C in freshwater systems, Geochim. Cosmochim. Acta 16 (1959) 15–38.
[46] E. Bard, B. Hamelin, R.G. Fairbanks, A. Zindler, Calibration of the ^{14}C timescale over the past 30,000 years using mass spectrometric U-Th ages from Barbados corals, Nature 345 (1990) 405–410.
[47] O. Joris, B. Weninger, Extension of the ^{14}C calibration curve to ca. 40,000 cal BC by synchronizing Greenland ^{18}O/^{16}O ice core records and North Atlantic foraminifera profiles: a comparison with U/Th coral data, Radiocarbon 40 (1998) 495–504.
[48] H. Kitagawa, J. van der Plicht, Atmospheric radiocarbon calibration to 45,000 yr B.P.: Late glacial fluctuations and cosmogenic isotope production, Science 279 (1998) 1187–1190.
[49] A.H.L. Voelker, P.M. Grootes, M.-J. Nadeau, M. Sarnthein, Radiocarbon levels in the Iceland Sea from 25–53 Kyr and their link to the Earth's magnetic field intensity, Radiocarbon 42 (2000) 437–452.
[50] A. Schramm, M. Stein, S.L. Goldstein, Calibration of the ^{14}C time scale to >40 ka by ^{234}U-^{230}Th dating of Lake Lisan sediments (last glacial Dead Sea), Earth Planet. Sci. Lett. 175 (2000) 27–40.
[51] J.W. Beck, D.A. Richards, R.L. Edwards, B.W. Silverman, P.L. Smart, D.J. Donahue, S. Herrera-Osterheld, G.S. Burr, L. Calsoyas, A.J.T. Jull, D. Biddulph, Extremely large variations of atmospheric ^{14}C concentration during the last glacial period, Science 292 (2001) 2453–2458.
[52] Y. Chen, P.E. Smith, N.M. Evensen, D. York, K.R. Lajoie, The edge of time: Dating young volcanic ash layers with the ^{40}Ar-^{39}Ar laser probe, Science 274 (1996) 1176–1178.
[53] J.N. Christensen, D.J. DePaolo, Time scales of large volume silicic magma systems – Sr isotopic systematics of phenocrysts and glass from the Bishop Tuff, Long Valley, California, Contrib. Mineral. Petrol. 113 (1993) 100–114.
[54] G.R. Davies, A.N. Halliday, G.A. Mahood, C.M. Hall, Isotopic constraints on the production rates, crystallization histories and residence times of pre-caldera silicic magmas, Long Valley, California, Earth Planet. Sci. Lett. 42 (1994) 444–450.
[55] P.E. Smith, N.M. Evensen, D. York, Under the volcano a new dimension in Ar-Ar dating of volcanic ash, Geophys. Res. Lett. 27 (2000) 585–588.
[56] T. Ton-That, B. Singer, M. Paterne, ^{40}Ar/^{39}Ar dating of latest Pleistocene (41 ka) marine tephra in the Mediterranean Sea implications for global climate records, Earth Planet. Sci. Lett. 184 (2001) 645–658.
[57] N.R. Nowaczyk, J. Knies, Magnetostratigraphic results from the eastern Arctic Ocean AMS ^{14}C ages and relative palaeointensity data of the Mono Lake and Laschamp geomagnetic reversal excursions, Geophys. J. Int. 140 (2000) 185–187.
[58] M. Frank, B. Schwarz, S. Baumann, P.W. Kubik, M. Suter, A. Mangini, A 200 kyr record of cosmogenic radionuclide production rate and geomagnetic field intensity

from ^{10}Be in globally stacked deep-sea sediments, Earth Planet. Sci. Lett. 149 (1997) 121–129.
[59] R.T. Merrill, M.W. McElhinny, P.L. McFadden, The Magnetic Field of the Earth: Paleomagnetism, the Core, and the Deep Mantle, Academic Press, San Diego, FL, 1996, 531 pp.
[60] H. Kitagawa, J. vanderPlicht, A 40,000-year varve chronology from Lake Suigetsu, Japan: Extension of the ^{14}C calibration curve, Radiocarbon 40 (1998) 505–515.
[61] B.D. Turrin, J.B. Donnelly-Nolan, B.C.J. Hearn, ^{40}Ar/^{39}Ar ages from the rhyolite of Alder Creek, California Age of the Cobb Mountain normal-polarity subchron revisited, Geology 22 (1994) 251–254.